PoS(LATTICE 2007)236
DESY 07-164
HU-EP-07/33
LMU-ASC 55/07

PROCEEDINGS OF SCIENCE

DESY 07-164
HU-EP-07/33
LMU-ASC 55/07

arXiv:0710.2565v1 [hep-lat] 14 Oct 2007

The chiral transition on a $24^3 \times 10$ lattice with $N_f = 2$ clover sea quarks studied by overlap valence quarks

Volker Weinberg[*] [a,b], **Ernst-Michael Ilgenfritz**[c], **Karl Koller**[d], **Yoshiaki Koma**[e], **Yoshifumi Nakamura**[a], **Gerrit Schierholz**[a,f], **Thomas Streuer**[g]

[a] *John von Neumann-Institut für Computing NIC, 15738 Zeuthen, Germany*
[b] *Institut für theoretische Physik, Freie Universität Berlin, 14196 Berlin, Germany*
[c] *Institut für Physik, Humboldt Universität zu Berlin, 12489 Berlin, Germany*
[d] *Sektion Physik, Universität München, 80333 München, Germany*
[e] *Numazu National College of Technology, Numazu 410-8501, Japan*
[f] *Deutsches Elektronen-Synchrotron DESY, 22603 Hamburg, Germany*
[g] *Dep. of Physics and Astronomy, University of Kentucky, Lexington, KY 40506-0055, USA*

E-Mail: *volker.weinberg@desy.de*

FOR THE DIK-COLLABORATION

Overlap fermions are particularly well suited to study the finite temperature dynamics of the chiral symmetry restoration transition of QCD, which might be just an analytic crossover. Using gauge field configurations on a $24^3 \times 10$ lattice with $N_f = 2$ flavours of dynamical Wilson-clover quarks generated by the DIK collaboration, we compute the lowest 50 eigenmodes of the overlap Dirac operator and try to locate the transition by fermionic means. We analyse the spectral density, local chirality and localisation properties of the low-lying modes and illustrate the changing topological and (anti-) selfdual structure of the underlying gauge fields across the transition.

The XXV International Symposium on Lattice Field Theory
July 30 - August 4, 2007
Regensburg, Germany

[*] Speaker.

© Copyright owned by the author(s) under the terms of the Creative Commons Attribution-NonCommercial-ShareAlike Licence.

1. Introduction and simulation parameters

Despite enormous theoretical efforts the very nature and order of the QCD finite temperature transition is still under debate and subject of current research (see e.g. [1] at this conference). To investigate confinement related aspects of the transition, during the last six years the DIK collaboration has generated dynamical configurations with $N_f = 2$ flavours of $O(a)$ improved Wilson sea quarks on a $16^3 \times 8$ lattice at $\beta = 5.2$ and 5.25 [2], a $24^3 \times 10$ lattice at $\beta = 5.20$ [3] and recently also a $24^3 \times 12$ lattice at $\beta = 5.29$ [4]. Based on the Polyakov loop susceptibility the critical temperature extrapolated to the continuum limit at physical m_π is determined as $r_0 T_c = 0.438(6)(^{+13}_{-7})$ [4].

Around three years ago we began to include the chiral symmetry breaking/restoration aspects of the QCD finite temperature transition to the topics of interest. Since overlap fermions implement exact chiral symmetry and the index theorem on the lattice, they are specially suited to study various chiral symmetry and topology related properties of the transition. First results using valence overlap fermions as a probe for dynamical $16^3 \times 8$ configurations at $\beta = 5.2$ were reported at LATTICE 2005 [5]. Meanwhile, we have developed a couple of tools based on the overlap Dirac operator and its eigenmodes and learned to use them for the investigation of the vacuum structure of quenched QCD at $T = 0$ [1].

In this paper we present results obtained by applying these methods in a hybrid approach to the $24^3 \times 10$ dynamical DIK configurations at finite T. We try to work out those signals which exhibit a remarkable difference between the low- and high-temperature phase of QCD. Using the Arnoldi algorithm we have computed the 50 lowest eigenvalues $i\lambda_i$ and eigenvectors $|\psi_i(x)\rangle$ (normalised as $\langle\psi_i|\psi_i\rangle = 1$) of the massless improved overlap operator $D(m_q = 0)$ for seven ensembles with κ values in the vicinity of the transition region. In [3] the critical value of κ marking the transition, κ_t, for this set of lattice configurations at fixed $\beta = 5.2$ has been determined from the peak of the Polyakov loop susceptibility χ_L shown in Fig. 1 (a) as $\kappa_t = 0.13542(6)$ and assigned to $r_0 T_c = 0.499(5)$ using interpolated QCDSF values for the Sommer parameter r_0/a found at $T = 0$. The number of configurations used in our overlap analysis together with the values for T/T_c and r_0/a are shown in Table 1.

κ	# confs	T/T_c	r_0/a
0.1348	131	0.91	4.561
0.1352	86	0.97	4.832
0.1353	131	0.98	4.902
0.1354	97	1.00	4.973
0.1355	118	1.01	5.045
0.1358	122	1.06	5.265
0.1360	97	1.09	5.417

Table 1: Simulation parameters for the configurations on the $24^3 \times 10$ lattice generated at $\beta = 5.2$.

[1] See [6] for a more detailed description of our tools and methods used throughout this paper.

2. Fermionic spectral approaches to locate the transition

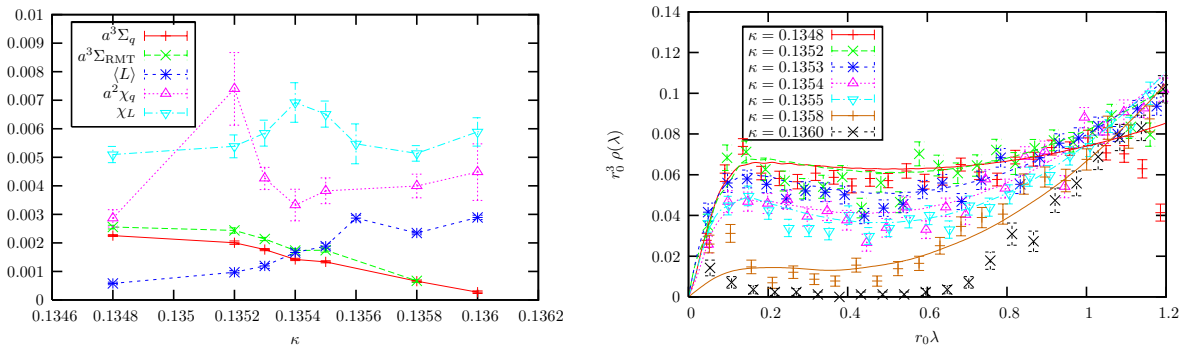

(a) (b)

Figure 1: (a) The Polyakov loop $\langle L\rangle$ and its susceptibility χ_L shown together with the chiral condensates $\Sigma_{q,\mathrm{RMT}}$ and the chiral susceptibility χ_q. $\Sigma_q(m_q)$ and χ_q are computed from the spectral representation of the chiral condensate using 50 eigenmodes, while Σ_{RMT} is obtained from the fits of the spectral density shown on the right. The two chiral condensates Σ_q and Σ_{RMT} agree quite well as functions of κ without further rescaling. To present the other curves in the same picture, they have been scaled appropriately. (b) The spectral densities $\rho(\lambda)$ together with fits using quenched random matrix theory predictions.

To determine the critical value of κ by fermionic means, we calculate the disconnected part of the chiral susceptibility $\chi_q = 1/V\ (\langle(\mathrm{Tr}\, D^{-1}(m_q))^2\rangle - \langle \mathrm{Tr}\, D^{-1}(m_q)\rangle^2)$ using a spectral decomposition of the chiral condensate $\Sigma_q(m_q) = 1/V\ \langle \mathrm{Tr}\, D^{-1}(m_q)\rangle = 1/V\ \langle \sum_i 1/(i\lambda_i + m_q)\rangle$. Truncating the decomposition acts as an UV-filter by removing short-distance fluctuations from the local condensate. We match the overlap valence and the Wilson sea quark masses by demanding that the corresponding pion masses be equal. The resulting quark masses range from $am_q = 0.045$ at $\kappa = 0.1348$ to $am_q = 0.006$ at $\kappa = 0.1360$. In Fig. 1 (a) one can see that χ_q shows a peak at $\kappa \approx 0.1352$. This value is significantly lower than $\kappa_t = 0.13542(6)$ as determined by the Polyakov loop susceptibility χ_L.

According to the Banks-Casher relation $\Sigma = -\pi\rho(0)$ the appearance of a gap in the spectrum is a criterion for a chiral symmetry restoring phase transition. We show in Fig. 1 (b) the spectral density $\rho(\lambda)$ of nonzero modes among the 50 lowest overlap operator eigenmodes for the seven analysed ensembles together with fits using quenched random matrix theory.[2] One can see that a gap in the spectrum does not appear below $\kappa \approx 0.1358$. As we have already observed on the $16^3 \times 8$ lattice [5], even for the highest analysed κ value some eigenvalues, which in fact exclusively belong to the first pair of nonzero modes, fall into the would-be gap.

Due to the hypothetic pinning-down of the lowest modes on singular confining defects [7] and their changing structure it is tempting to investigate the localisation properties of the low-lying modes. In Fig. 2 we plot for all considered ensembles the average Inverse Participation Ratio (IPR) $I = V\sum_x p_i(x)^2$, with the scalar density $p_i(x) = \langle \psi_i(x)|\psi_i(x)\rangle$, for λ_i in the respective bin. While the higher modes in the bulk of the spectrum are delocalised (*i.e.* have small IPR) in both phases, the zero modes and low-lying modes are strongly localised (*i.e.* have large IPR) in the

[2] Since the general formulae of RMT for $N_f = 2$ flavours converge to the quenched expressions for large quark masses, quenched RMT can be used as an approximation in the confined phase.

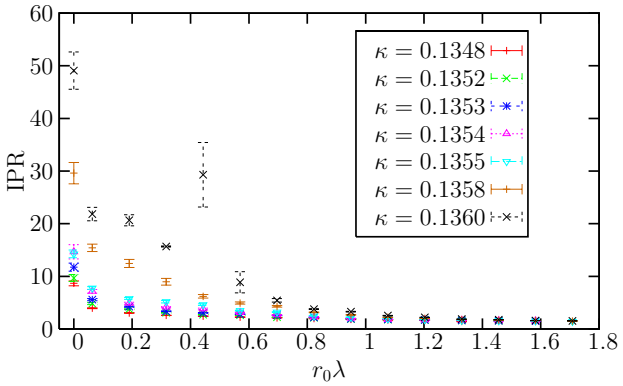

Figure 2: The average IPR for zero modes and for nonzero modes in bins of $r_0\lambda$ with a width 0.125.

confined phase. The transition is preceded by the lowest modes becoming even more localised before a gap finally opens. For the two largest κ-values the isolated modes which fall into the gap are extremely localised.

While the zero modes of the overlap operator are exactly chiral, *i.e.* $p_{5\,i}(x) := \langle\psi_i(x)|\gamma_5|\psi_i(x)\rangle = \pm p_i(x)$, the nonzero modes have globally vanishing chirality, $\sum_x p_{5\,i}(x) = 0$, but still exhibit a rich local chirality structure correlated with the underlying gauge fields. To visualise the changes of the local chirality of the nonzero modes in the vicinity of the transition, in Fig. 3 we show histograms of the local chirality variable characterising a mode at x, $X(x) = \frac{4}{\pi}\arctan\left(\sqrt{\frac{p_+(x)}{p_-(x)}}\right) - 1$ with $p_{\pm\,i}(x) = \langle\psi_i(x)|\frac{1}{2}(1\pm\gamma_5)|\psi_i(x)\rangle$ introduced in [8]. $X(x)$ clusters near ± 1 in the confined phase for the low modes when one selects lattice points near the peaks of the scalar density $p(x)$, signalling a high amount of local chirality. As λ increases, the signal for local chirality weakens. On the other hand, in the high-temperature phase the signal completely vanishes for modes outside the spectral gap. Only the modes which fall into the gap show a remanent strong local chirality.

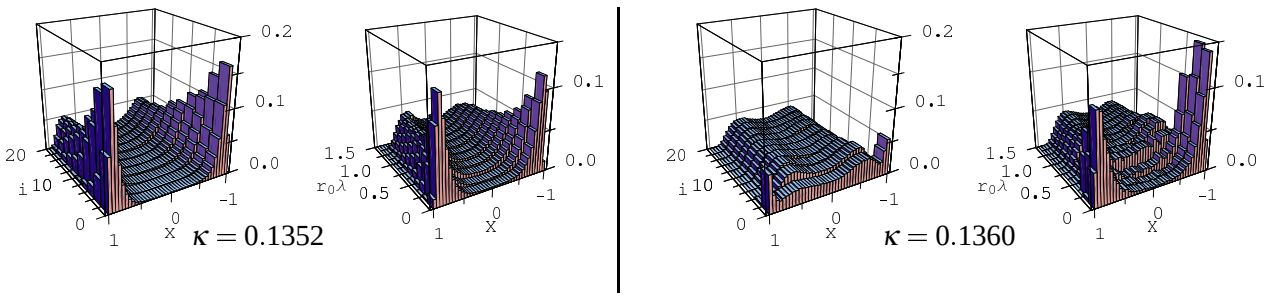

Figure 3: Normalised histograms of the local chirality $X(x)$ averaged over all configurations for $\kappa = 0.1352$ (left) and $\kappa = 0.1360$ (right). In both cases the left subpanel shows the chirality $X(x)$ for the lowest $i = 1,\ldots,20$ nonzero modes, whereas the right subpanel shows it for all nonzero modes averaged over bins in $r_0\lambda$ with bin width 0.125. Only 1 % of the lattice sites with largest scalar density $p(x)$ are considered.

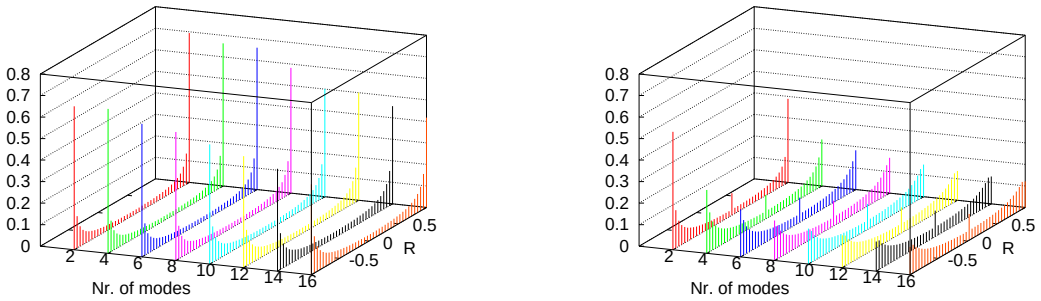

$\kappa = 0.1352$ $\kappa = 0.1360$

Figure 4: Normalised histograms with respect to the local (anti-)selfduality $X(x)$ of the UV-filtered field strength tensor in the $Q = 0$ subsample for $\kappa = 0.1352$ (left) and $\kappa = 0.1360$ (right) taken over all lattice sites in dependence of the number of nonzero modes included in the "filter".

Similar changes happen with the distribution of $R(x) = \frac{4}{\pi} \arctan r(x) - 1$, with $r(x) = (\tilde{s}(x) - \tilde{q}(x))/(\tilde{s}(x) + \tilde{q}(x))$, a measure proposed by Gattringer [9] to describe the local degree of (anti-) selfduality of the gluonic field strength tensor. Using a spectral decomposition of the gluonic field strength tensor, an UV-filtered version of the action density $\tilde{s}(x) = \sum_{i,j=1}^{n} \frac{\lambda_i^2 \lambda_j^2}{2} f^a_{\mu\nu}(x)_i f^a_{\mu\nu}(x)_j$ and of the charge density $\tilde{q}(x) = \sum_{i,j=1}^{n} \frac{\lambda_i^2 \lambda_j^2}{2} f^a_{\mu\nu}(x)_i \widetilde{f^a_{\mu\nu}(x)}_j$ (with $f^a_{\mu\nu}(x)_i = -\frac{i}{2} \langle \psi_i(x) | \gamma_\mu \gamma_\nu T^a | \psi_i(x) \rangle$) can be obtained from the overlap eigenmodes. $R(x)$ clusters near (+1) -1 for approximately (anti-)self-dual fields. In Fig. 4 we show that the contribution of the lowest modes to the spectral decomposition of the UV-filtered gluonic field strength tensor is highly (anti-)selfdual in the low-temperature phase, whereas in the high-temperature phase the coherence in the spectral decomposition which is necessary to build up an (anti-)selfdual UV-filtered field strength is almost completely lost.

Traditionally, the chiral symmetry restoration has been explained by pairing of instantons and antiinstantons. To describe the changes in the (anti-)selfdual structure in more detail and in a model-independent manner, we perform a cluster-analysis with respect to $R(x)$. Fig. 5 (a) shows the number of clusters consisting of link-connected sites x with $|R(x)| \geq R_{cut}$ as a function of the lower cutoff R_{cut}. One can see that for $\kappa < 0.1355$ in the confinement phase the number of clusters is surprisingly stable with increasing R_{cut}, whereas for the largest two κ values in the deconfined phase the number of clusters decreases rapidly towards large cutoffs, *i.e.* a high degree of (anti-) selfduality. In Fig. 5 (b) we show the connectivity $f(r_{max})$ of these clusters, *i.e.* the probability for two lattice points, separated by the maximal possible distance, to belong to the same cluster. Generally one can see that the larger the κ values are, the smaller this probability is. For the largest two κ values, percolation (*i.e.* $f(r_{max}) > 0$) completely disappears at $R_{cut} \approx 0.97$. Clusters that are more (anti-)selfdual than that are well isolated. On the other hand, in the low-temperature phase percolation exists almost up to $R_{cut} = 0.999$, indicating that perfectly (anti-)selfdual objects penetrate throughout the whole lattice volume. The average size of the largest cluster and the average size of all clusters, shown in Fig. 5 (c) and (d), respectively, as function of R_{cut} strongly decreases with higher temperatures.

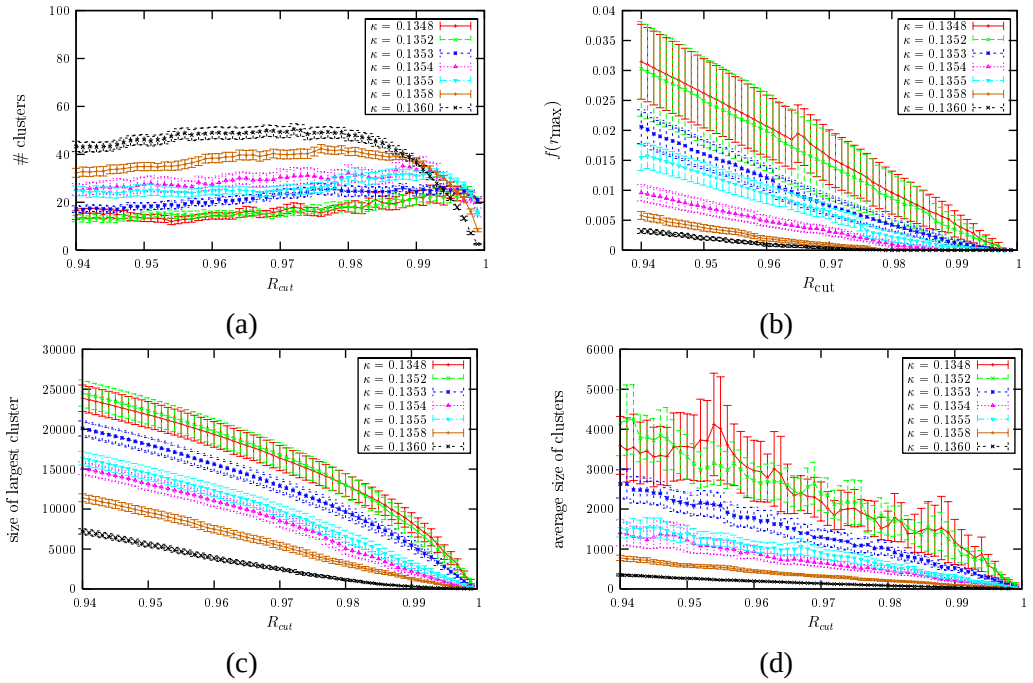

Figure 5: Results of the cluster analysis with respect to the local degree of (anti-)selfduality $R(x)$: (a) the number of clusters, (b) their connectivity, (c) the average size of the largest cluster and (d) the average size of all clusters, all as function of the cutoff R_{cut}.

3. Topological properties in the vicinity of the phase transition

Since overlap fermions offer an exact realisation of the Atiyah-Singer index theorem at finite cutoff a, the global topological charge is given as $Q = \sum_{i \in \text{ zeromodes}} \sum_x p_{5\,i}(x)$. The topological susceptibility $\chi_{top} = \langle Q^2 \rangle / V$ obtained from this fermionic definition of Q is displayed in Fig. 6 (a) and shows a rapid drop [3] in the analysed temperature interval $[0.91\ T_c, 1.09\ T_c]$. The susceptibility can be expressed as the integral $\chi_{top} = \int dx\, C_q(x)$ over the topological charge density correlator $C_q(x) = \langle q(0) q(x) \rangle$. Here we use the truncated eigenmode expansion of the topological charge density, $q_{IR}(x) = -\sum_{i=1}^{n} (1 - \frac{\lambda_i}{2})\ p_{5\,i}(x)$, including $n = 50$ eigenmodes in the "filter". The topological charge correlator $C_q(x)$ presented in Fig. 6 (b) shows a gradual change at the transition, revealing a short range charge compensation (traditionally interpreted as instanton-antiinstanton pairing) in the high-temperature phase.

4. Summary

We have complemented the efforts of the DIK collaboration to locate the confinement / deconfinement transition using gluonic signals (the Polyakov loop susceptibility) by a fermionic approach using valence overlap fermions as a probe. We observe that the chiral susceptibility shows a peak at a value $\kappa \approx 0.1352$ which is lower than $\kappa_t = 0.13542(6)$ as determined by the Polyakov loop method. On the other hand, a gap in the spectrum does not open below $\kappa \approx 0.1358$. The opening of the gap is preceded by the low-lying modes becoming more and more localised. When the gap

[3] The data for the lowest two κ values is likely to change with increased statistics. The Q-distributions (not shown here) for these two κ values exhibit strong deviation from Gaussian shape.

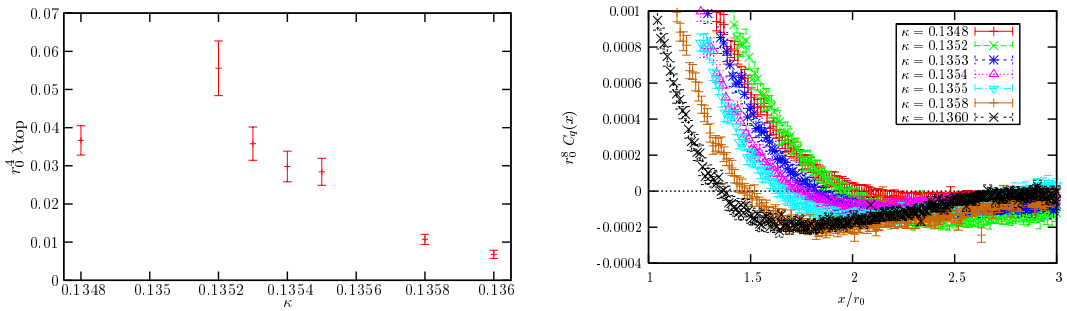

(a) (b)

Figure 6: (a) The topological susceptibility χ_{top} vs. κ. (b) The correlator $C_q(x)$ of the UV-filtered topological charge density computed from the lowest 50 eigenmodes. The plot focusses on the region where the correlator turns negative.

opens (apart from a few modes in the sample falling into the gap, which exclusively belong to the first pair of nonzero modes) the local chirality of the near-zero modes and the (anti-)selfduality which they contribute to the field strength tensor is almost completely lost. Only below $\kappa \approx 0.1358$ extended, approximately (anti-)selfdual domains (say with $R_{cut} \gtrapprox 0.97$) percolate throughout the whole lattice volume. The disappearance of such extended structures in the high-temperature phase is also reflected in the topological charge correlator, which signals some short-range charge compensation in the high-temperature phase. Thus it seems that different observables used to locate the transition yield different critical values for κ_t. This could be a hint that in $N_f = 2$ clover-improved QCD the finite temperature transition is realised as a crossover where various transition phenomena take place [10]. The nature of the real transition to the quark-gluon plasma remains an open question and requires further investigation.

Acknowledgements

The numerical overlap calculations have been performed on the IBM p690 at HLRN (Berlin). Part of this work is supported by DFG under contract FOR 465.

References

[1] Z. Fodor, PoS(LATTICE 2007)011; F. Karsch, PoS(LATTICE 2007)015.

[2] V. G. Bornyakov *et al.* [DIK Collaboration], *Phys. Rev.* **D71**, 114504 (2005) [hep-lat/0401014].

[3] V. G. Bornyakov *et al.* [DIK Collaboration], PoS(LAT2005)157.

[4] V. G. Bornyakov *et al.* [DIK Collaboration], PoS(LATTICE 2007)171.

[5] V. Weinberg *et al.*, PoS(LAT2005)171.

[6] E.-M. Ilgenfritz *et al.*, *Phys. Rev.* **D76**, 034506 (2007), 0705.0018 [hep-lat].

[7] E.-M. Ilgenfritz *et al.*, PoS(LATTICE 2007)311.

[8] I. Horvath *et al.*, *Phys. Rev.* **D65**, 014502 (2002), [hep-lat/0102003].

[9] C. Gattringer, *Phys. Rev. Lett.* **88**, 221601 (2002), [hep-lat/0202002].

[10] Y. Aoki *et al.*, Nature **443** (2006) 675, [hep-lat/0611014].